

# Motion Planning for Autonomous Vehicles: When Model Predictive Control Meets Ensemble Kalman Smoothing

Iman Askari<sup>1</sup>, Yebin Wang<sup>2</sup>, Vedang M. Deshpande<sup>2</sup>, and Huazhen Fang<sup>1</sup>

**Abstract**—Safe and efficient motion planning is of fundamental importance for autonomous vehicles. This paper investigates motion planning based on nonlinear model predictive control (NMPC) over a neural network vehicle model. We aim to overcome the high computational costs that arise in NMPC of the neural network model due to the highly nonlinear and nonconvex optimization. In a departure from numerical optimization solutions, we reformulate the problem of NMPC-based motion planning as a Bayesian estimation problem, which seeks to infer optimal planning decisions from planning objectives. Then, we use a sequential ensemble Kalman smoother to accomplish the estimation task, exploiting its high computational efficiency for complex nonlinear systems. The simulation results show an improvement in computational speed by orders of magnitude, indicating the potential of the proposed approach for practical motion planning.

## I. INTRODUCTION

Autonomous driving technologies have gained rapid advances in the past decade, showing significant promise in improving safety in transportation and access to mobility for diverse groups of people [1]. Motion planning is central to an autonomous vehicle, which is responsible for identifying the trajectories and maneuvers of the vehicle from a starting configuration to a goal configuration, while avoiding potential collisions and minimizing certain costs.

Various motion planning approaches have been proposed, ranging from graph-based methods such as Dijkstra and A\* search [2], [3] to sample-based approaches such as rapidly-exploring random trees and probabilistic roadmaps [4], [5]. However, they are often only suitable for small configuration spaces since their search times will increase exponentially with the dimension of the configuration space. Nonlinear model predictive control (NMPC) has emerged as a powerful alternative. By design, NMPC predicts the future behavior of a dynamic system and then finds the best control actions to optimize certain performance indices under input and state constraints. When applied to autonomous vehicles, NMPC can provide two crucial advantages [6]–[10]. First, it can continuously and predictively optimize motion plans to handle driving in a changing environment over a receding time horizon. Second, NMPC can incorporate the vehicle’s dynamics, physical limitations, and safety requirements into

This work was sponsored in part by the U.S. Army Research Laboratory under Cooperative Agreement Number W911NF-22-2-0207.

<sup>1</sup>I. Askari and H. Fang are with the Department of Mechanical Engineering, University of Kansas, Lawrence, KS 66045, USA. (Email: {askari, fang}@ku.edu)

<sup>2</sup>Y. Wang, and V. M. Deshpande are with the Mitsubishi Electric Research Laboratories, Cambridge, MA 02139, USA. (Email: {yebinwang, deshpande}@merl.com)

the online planning procedure, thus improving the safety and feasibility of planning.

The success of NMPC-based motion planning depends on the accuracy of the vehicle’s dynamic model. While physics-based vehicle modeling has been in wide use, practitioners often find it challenging to obtain accurate ones [11], [12]. Physical models are unable to capture the full range of various uncertain factors acting on a vehicle and often take a long time to develop due to the manual effort of theoretical analysis to experimental calibration. Data-driven machine learning has thus risen in recent years to enable vehicle modeling [13]. In particular, neural networks have found ever-increasing applications. The popularity of neural networks traces to their universal function approximation properties and their capabilities of using history information to grasp high-order or time-varying effects [11], [14]–[16].

However, NMPC of neural network models is non-trivial in terms of computational complexity. This is because NMPC must solve a constrained optimization problem in receding horizons. The implementation widely adopts gradient-based optimization solvers, but they struggle to perform a computationally efficient search for optima in the face of the nonlinear nonconvex neural network dynamics [11], [17]. The literature has presented some methods to mitigate the issue. A specially structured neural network is developed in [18] to facilitate the network’s integration with gradient-based NMPC, and an input-convex neural network is used in [19] to avoid nonconvex NMPC, which though comes at a sacrifice of the representation fidelity. The study in [17] exploits a random shooting technique for NMPC of neural networks in reinforcement learning tasks.

We have recently investigated the use of Bayesian estimation tools to solve NMPC of neural networks efficiently. In [9], we reformulate an NMPC problem as a Bayesian estimation problem that seeks to infer optimal control actions. Based on the reformulation, we use particle filtering/smoothing to address the estimation problem, exploiting its ability to perform sampling-based computation for fast search. Our further study in [10] applies the method to motion planning based on a neural network vehicle model. While our prior study shows the promise of using Bayesian estimation to address NMPC, the proposed approach has to perform forward filtering and then backward smoothing to estimate the optimal control actions. Also, we use the bootstrap particle filtering/smoothing technique in [10], which is easy to implement but still requires a large number of samples to achieve decent accuracy. These factors would limit the computational performance. We thus turn our attention to the ensemble Kalman filtering/smoothing. This

technique shares a similar structure with the standard Kalman filtering/smoothing but adopts Monte Carlo sampling-based implementation [20]. Its significant computational efficiency and suitability to high-dimensional nonlinear systems make it an appealing alternative to solve NMPC within the Bayesian estimation framework. We will use a sequential ensemble Kalman smoother (EnKS) characterized by a single forward-pass implementation [21]. As a recursive forward algorithm, this smoother avoids the two-pass smoothing, i.e., forward filtering and backward smoothing as in [10], to further speed up the computation. This will considerably facilitate motion planning, for which fast, real-time computation is crucial. To sum up, the core contribution of this study lies in developing a novel EnKS-based NMPC approach for autonomous vehicle motion planning. We also present various simulation results to validate the proposed approach.

The rest of the paper is organized as follows. Section II presents the NMPC-based motion planning problem. Section III then reformulates NMPC as a Bayesian estimation problem and develops the EnKS-based motion planning approach. Section IV offers simulation results to validate the proposed approach. Finally, Section V concludes the paper.

## II. NMPC MOTION PLANNING PROBLEM FORMULATION

To perform model-based motion planning, we use neural networks to capture the ego vehicle (EV) dynamics. Compared to first-principles vehicle modeling, neural networks are able to learn complex and non-transparent vehicle dynamics from abundant data and show excellent predictive accuracy even in the presence of uncertainty [16]. We thus consider a neural network-based vehicle model as follows:

$$\dot{x}_k = f_{\text{NN}}(x_k, u_k), \quad (1)$$

where  $f_{\text{NN}}(\cdot)$  represents a feedforward neural network,  $x_k$  is the state vector, and  $u_k$  is the control input vector. In above,  $x_k = [x_k^p \ y_k^p \ \psi_k \ \nu_k]^\top$ , where  $(x_k^p, y_k^p)$  is the EV's position in the global coordinates,  $\psi_k$  is the heading angle, and  $\nu_k$  is the speed;  $u_k = [a_k \ \delta_k]^\top$ , where  $a_k$  is the vehicle's acceleration, and  $\delta_k$  is the front wheel's steering angle. We discretize the model in (1) as below for the purpose of computation in motion planning:

$$x_{k+1} = f(x_k, u_k) = x_k + \Delta t \cdot f_{\text{NN}}(x_k, u_k), \quad (2)$$

where  $\Delta t$  is the sampling period.

The EV should never collide with its surrounding obstacle vehicles (OVs). At time  $k$ , we denote the state of the EV as  $x_k^{\text{EV}}$  and the state of the  $i$ -th OV as  $x_k^{\text{OV},i}$  for  $i = 1, \dots, M_O$ , where  $M_O$  is the number of OVs. To prevent collisions, the EV must maintain a safe distance from all OVs. This requirement can be expressed as:

$$d(x_k^{\text{EV}}, x_k^{\text{OV},i}) \geq d_{\min}, \quad i = 1, \dots, M_O, \quad (3)$$

where  $d(\cdot, \cdot)$  represents the distance between the vehicles characterized by their shape, and  $d_{\min}$  is the minimum safe distance. The EV is assumed to be driven on a structured road and expected to stay within the road's boundaries. This requirement is met by imposing the following constraint:

$$d_B(x_k) \leq L, \quad (4)$$

where  $d_B(x_k) = \|x_k - B\|_2$ ,  $B$  is the closest point from the road boundary to the EV, and  $L$  is the road's width. The EV's acceleration and steering control inputs are limited due to both the actuation limits and the need to ensure passenger comfort. This implies

$$u_{\min} \leq u_k \leq u_{\max}, \quad (5)$$

where  $u_{\min}$  and  $u_{\max}$  are the lower and upper control bounds. To simplify the notation, we summarize the planning constraints (3)-(5) compactly as follows:

$$g(x_k, u_k) \leq 0. \quad (6)$$

With the above formulation, we are now ready to formulate the NMPC motion planning problem. The problem setup should not only include the above constraints but also reflect the general driving requirements. We expect the EV to track a nominal reference path, penalize actuation costs, and comply with the safety constraints. The corresponding NMPC problem is stated as follows:

$$\min \sum_{t=k}^{k+H} (x_t - r_t)^\top R(x_t - r_t) + u_t^\top Qu_t, \quad (7a)$$

$$\text{s.t. } (2), (6), \quad t = k, \dots, k + H, \quad (7b)$$

where  $H$  is the prediction planning horizon length,  $Q$  and  $R$  are weight matrices, and collectively the optimization variables are  $\{x_{k:k+H}, u_{k:k+H}\}$ , where  $x_{k:k+H} = \{x_k, \dots, x_{k+H}\}$ . The reference path  $r_{k:k+H}$  is composed of a sequence of waypoints given by a higher decision-making module. The motion planner solves the problem in (7) at every time  $k$  to obtain  $u_{k:k+H}^*$  and applies the first element  $u_k^*$  to drive the EV to the next state  $x_{k+1}$ . The planner then repeats the procedure in receding horizons.

Traditional solvers for the problem in (7) are based on gradient-based optimization. However, they would struggle to compute solutions efficiently here. The neural network-based model will make the optimization landscapes extremely nonlinear and nonconvex, to hinder efficient search. As will be shown in Section IV, the computational time by gradient-based optimization is almost formidable. Therefore, we will pursue an alternative method that is more competent in computation, which translates the NMPC problem in (7) into a Bayesian estimation problem and then harnesses the highly efficient EnKS to perform the estimation.

## III. MOTION PLANNING VIA ENKS-BASED NMPC

This section presents the main results, showing the development of an EnKS-based NMPC for motion planning.

### A. Setup of NMPC as Bayesian Estimation

Given the NMPC problem in (7), we can view the control objective as evidence and then infer the best control actions given the evidence. This perspective motivates us to set up a Bayesian estimation problem with equivalence to (7). To show the estimation problem, we begin by considering the following virtual system:

$$x_{t+1} = f(x_t, u_t), \quad (8a)$$

$$u_{t+1} = w_t, \quad (8b)$$

$$r_t = x_t + v_t, \quad (8c)$$

for  $k \leq t \leq k+H$ , where  $w_t$  and  $v_t$  are additive noises. For now, it is our interest to consider the state estimation problem for (8) from the viewpoint of probabilistic inference. Following the principle of maximum a posterior estimation, the following problem is of our interest:

$$\max_{x_{k:k+H}, u_{k:k+H}} \log p(x_{k:k+H}, u_{k:k+H} | r_{k:k+H}). \quad (9)$$

This estimation problem holds an equivalence to the NMPC problem in (7) under some conditions [10].

*Theorem 1:* Assume that  $w_t$  and  $v_t$  are independent white noises with  $w_t \sim \mathcal{N}(0, Q^{-1})$  and  $v_t \sim \mathcal{N}(0, R^{-1})$ . Then, the problems in (7) and (9) have the same optima if neglecting (6).

*Proof:* By the Markovian property of (8) and Bayes' rule, we have

$$p(x_{k:k+H}, u_{k:k+H} | r_{k:k+H}) \propto \prod_{t=k}^{k+H} p(r_t | x_t) p(u_t) \cdot \prod_{t=k}^{k+H-1} p(x_{t+1} | x_t, u_t) p(x_k).$$

As (8a) is deterministic and the initial state  $x_k$  is known, the above reduces to

$$p(x_{k:k+H}, u_{k:k+H} | r_{k:k+H}) \propto \prod_{t=k}^{k+H} p(r_t | x_t) p(u_t).$$

This implies that

$$\begin{aligned} \log p(x_{k:k+H}, u_{k:k+H} | r_{k:k+H}) \\ \propto \sum_{t=k}^{k+H} \log p(r_t | x_t) + \log p(u_t). \end{aligned}$$

As  $p(r_t | x_t) \sim \mathcal{N}(x_t, R^{-1})$  and  $p(u_t) \sim \mathcal{N}(0, Q^{-1})$ , we have

$$\begin{aligned} \log p(r_t | x_t) &\propto -(x_t - r_t)^\top R(x_t - r_t), \\ \log p(u_t) &\propto -u_t^\top Qu_t. \end{aligned}$$

Combining the above, we see that problem (9) can be expressed as

$$\min_{x_{k:k+H}, u_{k:k+H}} \sum_{t=k}^{k+H} (x_t - r_t)^\top R(x_t - r_t) + u_t^\top Qu_t,$$

which is the same as problem (7) without the constraint in (6). The theorem is thus proven. ■

*Theorem 1* indicates the viability of leveraging Bayesian estimation to solve the original motion planning problem in (7), whereby one would estimate the best control actions and motion plans based on the planning objectives.

Proceeding further, we must embed (9) with the constraint in (6). To this end, we introduce a virtual measurement  $z_t$ :

$$z_t = \phi(g(x_t, u_t)) + \eta_t. \quad (10)$$

Here,  $\phi(\cdot)$  is a barrier function, which outputs zero when the constraint is satisfied and infinity otherwise, and  $\eta_t \sim \mathcal{N}(0, R_\eta)$  is a small additive noise. It is seen that  $z_t$  should

take zero to ensure constraint satisfaction. We choose  $\phi(\cdot)$  to be a softplus function for the sake of numerical computation:

$$\phi(s) = \frac{1}{\alpha} \ln(1 + \exp(\beta s)), \quad (11)$$

where the tunable parameters  $\alpha$  and  $\beta$  determine how strict to implement the constraint.

For notational simplicity, we rewrite the virtual system in (8) along with  $z_t$  in the following augmented form:

$$\bar{x}_{t+1} = \bar{f}(\bar{x}_t) + \bar{w}_t, \quad (12a)$$

$$\bar{y}_t = \bar{h}(\bar{x}_t) + \bar{v}_t, \quad (12b)$$

where

$$\begin{aligned} \bar{x}_t &= \begin{bmatrix} x_t \\ u_t \end{bmatrix}, \quad \bar{y}_t = \begin{bmatrix} r_t \\ z_t \end{bmatrix}, \quad \bar{w}_t = \begin{bmatrix} 0 \\ w_t \end{bmatrix}, \\ \bar{v}_t &= \begin{bmatrix} v_t \\ \eta_t \end{bmatrix}, \quad \bar{f}(\bar{x}_t) = \begin{bmatrix} f(x_t, u_t) \\ 0 \end{bmatrix}, \quad \bar{h}(\bar{x}_t) = \begin{bmatrix} x_t \\ \phi(g(x_t, u_t)) \end{bmatrix}. \end{aligned}$$

Given (12), we will focus on Bayesian state estimation to find out the best  $\bar{x}^*$  in line of (9) by considering  $p(\bar{x}_{k:k+H} | \bar{y}_{k:k+H})$ . This is known as a smoothing problem. While various computational algorithms are available to address it, we are particularly interested in ensemble Kalman estimation because of their high computational efficiency and performance in handling nonlinearity. In the sequel, we will show a sequential EnKS algorithm to enable computationally fast estimation for (12).

### B. Sequential Ensemble Kalman Smoothing

Ensemble Kalman estimation traces its origin to Monte Carlo simulation. Characteristically, it approximates concerned probability distributions by ensembles of samples and updates the ensembles in a Kalman-update manner when new data are available. Combining the essences of Monte Carlo sampling and Kalman filtering, it can handle strong nonlinearity in high-dimensional state spaces and compute fast. There are different ways to do smoothing in terms of ensemble Kalman estimation. In this study, we choose a sequential EnKS approach in [21] to address the estimation problem in Section III-A. This approach sequentially updates the ensembles for all the past states at every time upon the arrival of new data. As such, it performs smoothing in a single forward pass to save much computation compared to the two pass smoothing methods, thus advantageous for our motion planning estimation task.

Consider  $p(\bar{x}_{k:t} | \bar{y}_{k:t})$  for an arbitrary  $t \in [k, \dots, k+H]$ . For notational convenience, we drop the subscript  $k$  and define  $\mathcal{X}_t = \bar{x}_{k:t}$  and  $\mathcal{Y}_t = \bar{y}_{k:t}$ . Then, using Bayes' rule, we have the following recursive relation:

$$p(\mathcal{X}_t | \mathcal{Y}_t) \propto p(\bar{y}_t | \bar{x}_t) p(\bar{x}_t | \bar{x}_{t-1}) p(\mathcal{X}_{t-1} | \mathcal{Y}_{t-1}). \quad (13)$$

At time  $t-1$ , we assume

$$\begin{aligned} p\left(\begin{bmatrix} \mathcal{X}_t \\ \bar{y}_t \end{bmatrix} \mid \mathcal{Y}_{t-1}\right) &\sim \\ \mathcal{N}\left(\begin{bmatrix} \hat{\mathcal{X}}_{t|t-1} \\ \hat{\bar{y}}_{t|t-1} \end{bmatrix}, \begin{bmatrix} \mathcal{P}_{t|t-1}^{\mathcal{X}} & \mathcal{P}_{t|t-1}^{\mathcal{X}, \bar{y}} \\ (\mathcal{P}_{t|t-1}^{\mathcal{X}, \bar{y}})^\top & \mathcal{P}_{t|t-1}^{\bar{y}} \end{bmatrix}\right), \quad (14) \end{aligned}$$

where  $\hat{\mathcal{X}}$  and  $\hat{y}$  are the means for  $\mathcal{X}$  and  $\bar{y}$ , respectively, and  $\mathcal{P}$  represents the covariances (or cross-covariances). It then follows that

$$p(\mathcal{X}_t | \mathcal{Y}_t) \sim \mathcal{N} \left( \hat{\mathcal{X}}_{t|t}, \mathcal{P}_{t|t}^{\mathcal{X}} \right), \quad (15)$$

where

$$\hat{\mathcal{X}}_{t|t} = \hat{\mathcal{X}}_{t|t-1} + \mathcal{P}_{t|t-1}^{\mathcal{X}, \bar{y}} \left( \mathcal{P}_{t|t-1}^{\bar{y}} \right)^{-1} \left( \bar{y}_t - \hat{y}_{t|t-1} \right), \quad (16a)$$

$$\mathcal{P}_{t|t}^{\mathcal{X}} = \mathcal{P}_{t|t-1}^{\mathcal{X}} - \mathcal{P}_{t|t-1}^{\mathcal{X}, \bar{y}} \left( \mathcal{P}_{t|t-1}^{\bar{y}} \right)^{-1} \left( \mathcal{P}_{t|t-1}^{\mathcal{X}, \bar{y}} \right)^{\top}. \quad (16b)$$

When  $t$  moves from  $k$  to  $k+H$ , the smoothing process is completed for the considered horizon.

To realize the above procedure, we approximately represent  $p(\mathcal{X}_{t-1} | \mathcal{Y}_{t-1})$  by an ensemble of samples  $\mathcal{X}_{t-1|t-1}^i$  for  $i = 1, \dots, N$  with mean  $\hat{\mathcal{X}}_{t-1|t-1}$  and covariance  $\mathcal{P}_{t-1|t-1}^{\mathcal{X}}$ . Then, we pass  $\bar{x}_{t-1|t-1}^i$  through (12a) to obtain the ensemble that approximates  $p(\bar{x}_t | \mathcal{Y}_{t-1})$ :

$$\bar{x}_{t|t-1}^i = \bar{f}(\bar{x}_{t-1|t-1}^i) + \bar{w}_{t-1}^i, \quad i = 1, \dots, N, \quad (17)$$

where  $\bar{w}_{t-1}^i$  are samples drawn from  $\mathcal{N}(0, \text{diag}(0, Q^{-1}))$ . The corresponding sample mean and covariance can be calculated as

$$\hat{\bar{x}}_{t|t-1} = \frac{1}{N} \sum_{i=1}^N \bar{x}_{t|t-1}^i, \quad (18a)$$

$$\mathcal{P}_{t|t-1}^{\bar{x}} = \frac{1}{N-1} \sum_{i=1}^N \left( \bar{x}_{t|t-1}^i - \hat{\bar{x}}_{t|t-1} \right) \left( \bar{x}_{t|t-1}^i - \hat{\bar{x}}_{t|t-1} \right)^{\top}, \quad (18b)$$

Then, we concatenate  $\bar{x}_{t|t-1}^i$  and  $\hat{\bar{x}}_{t|t-1}$  with  $\mathcal{X}_{t-1|t-1}^i$  and  $\hat{\mathcal{X}}_{t-1|t-1}$ , respectively, to create  $\mathcal{X}_{t|t-1}^i \leftarrow (\mathcal{X}_{t-1|t-1}^i, \bar{x}_{t|t-1}^i)$  and  $\hat{\mathcal{X}}_{t|t-1} \leftarrow (\hat{\mathcal{X}}_{t-1|t-1}, \hat{\bar{x}}_{t|t-1})$ . The covariance for  $p(\mathcal{X}_t | \mathcal{Y}_{t-1})$  is constructed as

$$\mathcal{P}_{t|t-1}^{\mathcal{X}} = \begin{bmatrix} \mathcal{P}_{t-1|t-1}^{\mathcal{X}} & \mathcal{P}_{t|t-1}^{\mathcal{X}, \bar{x}} \\ \left( \mathcal{P}_{t|t-1}^{\mathcal{X}, \bar{x}} \right)^{\top} & \mathcal{P}_{t|t-1}^{\bar{x}} \end{bmatrix}, \quad (19)$$

where

$$\mathcal{P}_{t|t-1}^{\mathcal{X}, \bar{x}} = \frac{1}{N-1} \sum_{i=1}^N \left( \mathcal{X}_{t-1|t-1}^i - \hat{\mathcal{X}}_{t-1|t-1} \right) \left( \bar{x}_{t|t-1}^i - \hat{\bar{x}}_{t|t-1} \right)^{\top}.$$

To approximate  $p(\bar{y}_t | \mathcal{Y}_{t-1})$ , we construct an ensemble of samples by

$$\bar{y}_{t|t-1}^i = \bar{h}(\bar{x}_{t|t-1}^i) + \bar{v}_t^i, \quad i = 1, \dots, N, \quad (20)$$

where  $\bar{v}_t^i$  are drawn from  $\mathcal{N}(0, \text{diag}(R^{-1}, R_{\eta}))$ . The sample mean, and covariance of the measurement ensemble is

$$\hat{y}_{t|t-1} = \frac{1}{N} \sum_{i=1}^N \bar{y}_{t|t-1}^i, \quad (21a)$$

$$\mathcal{P}_{t|t-1}^{\bar{y}} = \frac{1}{N-1} \sum_{i=1}^N \left( \bar{y}_{t|t-1}^i - \hat{y}_{t|t-1} \right) \left( \bar{y}_{t|t-1}^i - \hat{y}_{t|t-1} \right)^{\top}. \quad (21b)$$

**Algorithm 1** Ensemble Kalman Motion Planner: the motion planner based on NMPC realized by EnKS.

---

```

1: Set up the NMPC motion planning problem as in (7)
2: Convert the problem to its Bayesian estimation counterpart as in (12)
3: for  $k = 1, \dots, T$  do
4:   for  $t = k, \dots, k+H$  do
5:     if  $t = k$  then
6:       if  $k = 1$  then
7:         Draw samples  $\bar{x}_k^i \sim p(\bar{x}_k)$ ,  $i = 1, \dots, N$ 
8:       else
9:         Warmstart  $\bar{x}_k^i$  using  $\bar{x}_{t+1}^i$  from  $\mathcal{X}_{k+H|k+H}^i$  at time  $k-1$ 
10:      end if
11:    end if
12:    Generate  $\bar{x}_{t|t-1}^i$  using (17)
13:    Compute  $\hat{\bar{x}}_{t|t-1}$  and  $\mathcal{P}_{t|t-1}^{\bar{x}}$  via (18a)-(18b)
14:    Concatenate  $\mathcal{X}_{t|t-1}^i \leftarrow (\mathcal{X}_{t-1|t-1}^i, \bar{x}_{t|t-1}^i)$ 
15:    Concatenate  $\hat{\mathcal{X}}_{t|t-1} \leftarrow (\hat{\mathcal{X}}_{t-1|t-1}, \hat{\bar{x}}_{t|t-1})$ 
16:    Compute  $\mathcal{P}_{t|t-1}^{\mathcal{X}}$  via (19)
17:    Generate  $\bar{y}_{t|t-1}^i$  using (20)
18:    Compute  $\hat{y}_{t|t-1}^i$  and  $\mathcal{P}_{t|t-1}^{\bar{y}}$  via (21a)-(21b)
19:    Compute  $\mathcal{P}_{t|t-1}^{\mathcal{X}, \bar{y}}$  via (22)
20:    Obtain updated samples  $\mathcal{X}_{t|t}^i$  using (23)
21:    Compute  $\hat{\mathcal{X}}_{t|t}$  and  $\mathcal{P}_{t|t}^{\mathcal{X}}$  via (24a)-(24b)
22:  end for
23:  Extract the estimated control  $u_k^*$  from  $\hat{\mathcal{X}}_{k+H|k+H}$ 
24: end for

```

---

Then, the cross-covariance between  $\mathcal{X}_t$  and  $\bar{y}_t$  is found by

$$\mathcal{P}_{t|t-1}^{\mathcal{X}, \bar{y}} = \frac{1}{N-1} \sum_{i=1}^N \left( \mathcal{X}_{t|t-1}^i - \hat{\mathcal{X}}_{t|t-1} \right) \left( \bar{y}_{t|t-1}^i - \hat{y}_{t|t-1} \right)^{\top}. \quad (22)$$

Based on (16),  $\mathcal{X}_{t|t-1}^i$  can be updated individually as

$$\mathcal{X}_{t|t}^i = \mathcal{X}_{t|t-1}^i + \mathcal{P}_{t|t-1}^{\mathcal{X}, \bar{y}} \left( \mathcal{P}_{t|t-1}^{\bar{y}} \right)^{-1} \left( \bar{y}_t - \bar{y}_{t|t-1}^i \right). \quad (23)$$

Finally, the smoothed estimate and the associated covariance are given by

$$\hat{\mathcal{X}}_{t|t} = \frac{1}{N} \sum_{i=1}^N \mathcal{X}_{t|t}^i, \quad (24a)$$

$$\mathcal{P}_{t|t}^{\mathcal{X}} = \frac{1}{N-1} \sum_{i=1}^N \left( \mathcal{X}_{t|t}^i - \hat{\mathcal{X}}_{t|t} \right) \left( \mathcal{X}_{t|t}^i - \hat{\mathcal{X}}_{t|t} \right)^{\top}. \quad (24b)$$

The EnKS is outlined in (17)-(24). This approach is characterized by sequential computation in one pass. Compared to two-pass smoothers in the literature, it presents higher computational efficiency and thus is a favorable choice for addressing our estimation problem for motion planning. Note that the execution of (18b), (19), and (24b) can be skipped to speed up the computation further if one has no interest in computing the covariances for the quantification of the uncertainty in estimation. Based on the outlined EnKS approach, we can solve the NMPC-based motion planning problem and propose the Ensemble Kalman Motion Planner as summarized in Algorithm 1.

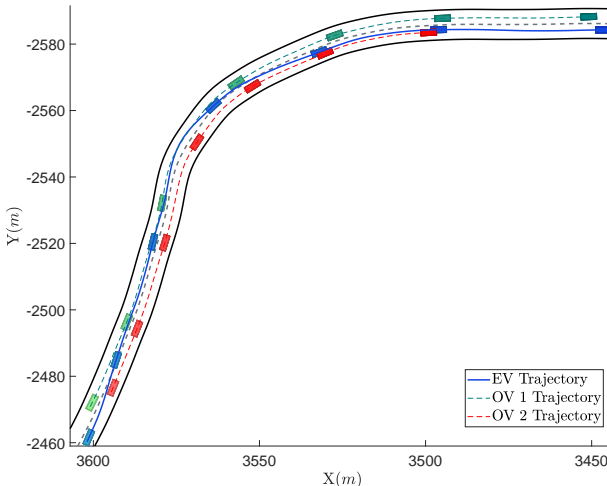


Fig. 1: Vehicle trajectories and positions during the simulation. The EV performing EnKS motion planning is denoted in blue. The other green and red vehicles are OVs. The color gradient from light to dark represents the vehicle's position from the past to the future.

#### IV. NUMERICAL SIMULATION

In this section, we apply the Ensemble Kalman Motion Planner to motion planning when the EV is set to overtake the slow-moving OVs on a curved road. The trained neural network consists of two hidden layers with 128 neurons in each layer and is trained using the Adam optimizer. We generated the training data using the single-track bicycle model in [22]. The sampling period  $\Delta t$  is 0.1 s.

In Fig. 1, we depict the movement of the blue-colored EV and two OVs in green and red. All the vehicles start from the left and travel to the right along the curved road. The motion planner must help the EV find the best path and actuation to accomplish the overtaking task safely on the curved road. The EV can always find a safe trajectory forward using the proposed Ensemble Kalman Motion Planner, as shown in Fig. 2. We also evaluate the effects of the ensemble size  $N$  on the estimated control profiles, as illustrated in Figs. 2a-2b. The increase in sample size results in more accurate estimation and smoother control profiles while meeting the driving constraints, as is seen. Further, the distances between the EV and OVs are plotted in Fig. 2c when  $N = 200$ , depicting the capability of the Ensemble Kalman Motion Planner to always maintain a safe distance between the EV and OVs.

As discussed earlier, the Ensemble Kalman Motion Planner is designed for fast computation. We thus evaluate its computational performance as well as its cost performance through a comparison with gradient-based optimization. The simulations run on a workstation equipped with an Intel i9-10920X 3.5 GHz CPU and 128 GB of RAM. For gradient-based optimization, we used MATLAB's 2023a MPC Toolbox with the default interior-point algorithm and computed the expressions of the gradients offline for the optimization run.

In Fig. 3, we compare the cost value for the Ensemble Kalman Motion Planner and gradient-based optimiza-

TABLE I: Numerical comparison of EnKS and optimization

Horizon ( $H$ )	Method	Total Cost	Average Computation Time (s)	Relative Cost Change (%)	Relative Computation Time Change (%)
40	Optimization	14,680	54.92	—	—
	EnKS ( $N = 50$ )	17,853	0.158	21.6	-99.71
	EnKS ( $N = 100$ )	16,126	0.242	9.85	-99.56
	EnKS ( $N = 200$ )	15,102	0.366	2.88	-99.61
60	Optimization	—	143.3	—	—
	EnKS ( $N = 50$ )	18,845	0.250	—	-99.83
	EnKS ( $N = 100$ )	17,655	0.385	—	-99.73
	EnKS ( $N = 200$ )	15,798	0.561	—	-99.61

tion motion planner for  $H = 40$  and  $H = 60$ . When  $H = 40$ , the Ensemble Kalman Motion Planner has comparable cost performance with gradient-based optimization. On the contrary, when  $H = 60$ , gradient-based optimization fails due to the increase in nonconvexity and size of the optimization problem, while the Ensemble Kalman Motion Planner is successful because of its sequential formulation and ability to handle high-dimensional nonlinear Bayesian state estimation problems.

In Table I, we report the numerical comparison between both approaches when the prediction horizon  $H = 40$  and 60 and when the Ensemble Kalman Motion Planner's ensemble size  $N$  is 50, 100 and 200. Additionally, we have numerically summarized the cost attained by each approach during the simulation time interval  $0 \leq k \leq 500$ . The relative cost achieved by the Ensemble Kalman Motion Planner compared to gradient optimization when  $H = 40$  and  $N = 200$  is 2% higher than optimization, which is acceptable considering the computational efficiency. In all the cases, the Ensemble Kalman Motion Planner has remarkable computational efficiency, which is faster by orders of magnitude compared with gradient optimization, having a relative decrease of over 99%. Again, note that gradient optimization fails when  $H = 60$  and requires almost unmanageable computational times even with shorter prediction horizons from a practical viewpoint. By contrast, the Ensemble Kalman Motion Planner still demonstrates very fast speed, showing its desired capability of enabling long prediction horizons and good scalability with the number of optimization variables involved in planning.

#### V. CONCLUSION

Autonomous vehicles rely on high-performance motion planning to achieve their full potential. In this paper, we consider the design of a motion planner that uses neural networks to predict a vehicle's dynamics and exploits NMPC to compute safe, optimal trajectories. However, the planner will suffer from high computational complexity if adopting gradient-based solvers, as the neural network model will make the underlying optimization problem highly nonlinear and nonconvex. We show that a sequential EnKS approach can approximately implement the NMPC-based motion planner with very fast computation. What makes this design possible is the reformulation of NMPC as a Bayesian estimation problem. In the simulations, the proposed Ensemble Kalman Motion Planner shows itself to be faster than gradient-based optimization by orders of magnitude.

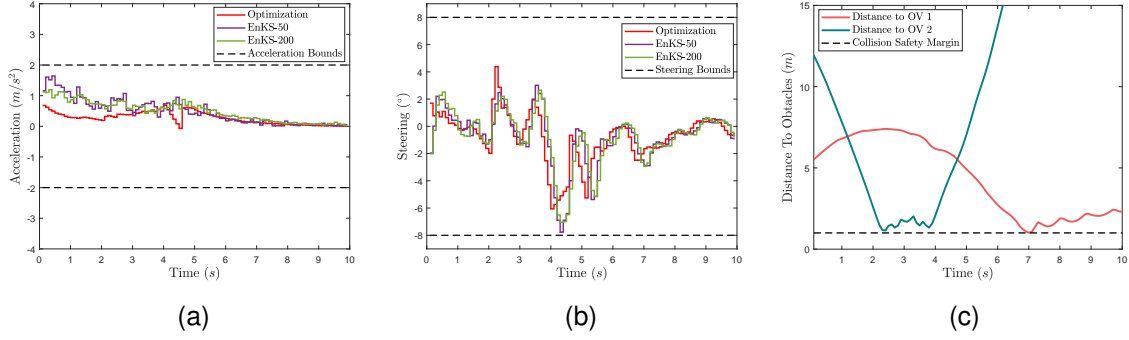


Fig. 2: The control profile and constraint satisfaction by the EV running optimization and Ensemble Kalman Motion Planner. (a) Acceleration control profiles with respective bounds. (b) Steering control profiles with respective bounds. (c) Distance between the EV and OVs when  $N = 200$  with a safety margin of 1 m.

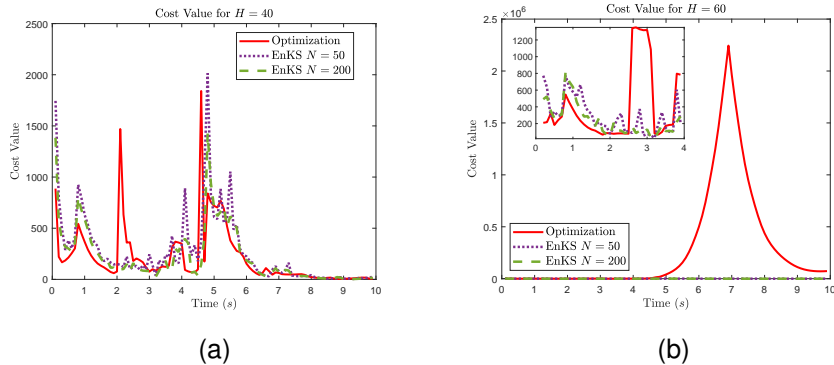


Fig. 3: Cost comparison over the simulation time between optimization and EnKS with different particle numbers for two horizon lengths. (a)  $H = 40$ . (b)  $H = 60$ .

## REFERENCES

- [1] M. Woldeamanuel and D. Nguyen, "Perceived benefits and concerns of autonomous vehicles: An exploratory study of millennials' sentiments of an emerging market," *Research in Transportation Economics*, vol. 71, pp. 44–53, 2018.
- [2] E. W. Dijkstra, "A note on two problems in connexion with graphs," *Numerische Mathematik*, vol. 1, no. 1, pp. 269–271, 1959.
- [3] P. E. Hart, N. J. Nilsson, and B. Raphael, "A formal basis for the heuristic determination of minimum cost paths," *IEEE Transactions on Systems Science and Cybernetics*, vol. 4, no. 2, pp. 100–107, 1968.
- [4] S. M. LaValle, "Rapidly-exploring random trees: a new tool for path planning," *The annual research report*, 1998.
- [5] L. Kavraki, P. Svestka, J.-C. Latombe, and M. Overmars, "Probabilistic roadmaps for path planning in high-dimensional configuration spaces," *IEEE Transactions on Robotics and Automation*, vol. 12, no. 4, pp. 566–580, 1996.
- [6] V. Turri, A. Carvalho, H. E. Tseng, K. H. Johansson, and F. Borrelli, "Linear model predictive control for lane keeping and obstacle avoidance on low curvature roads," in *16th International IEEE Conference on Intelligent Transportation Systems*, 2013, pp. 378–383.
- [7] N. Murgovski and J. Sjöberg, "Predictive cruise control with autonomous overtaking," in *54th IEEE Conference on Decision and Control*, 2015, pp. 644–649.
- [8] J. Ji, A. Khajepour, W. W. Melek, and Y. Huang, "Path planning and tracking for vehicle collision avoidance based on model predictive control with multiconstraints," *IEEE Transactions on Vehicular Technology*, vol. 66, no. 2, pp. 952–964, 2017.
- [9] I. Askari, S. Zeng, and H. Fang, "Nonlinear model predictive control based on constraint-aware particle filtering/smoothing," in *American Control Conference*, 2021, pp. 3532–3537.
- [10] I. Askari, B. Badnava, T. Woodruff, S. Zeng, and H. Fang, "Sampling-based nonlinear MPC of neural network dynamics with application to autonomous vehicle motion planning," in *American Control Conference*, 2022, pp. 2084–2090.
- [11] A. Draeger, S. Engell, and H. Ranke, "Model predictive control using neural networks," *IEEE Control Systems Magazine*, vol. 15, no. 5, pp. 61–66, 1995.
- [12] S. Piché, J. Keeler, G. Martin, G. Boe, D. Johnson, and M. Gerules, "Neural network based model predictive control," in *Proceedings of the 12th International Conference on Neural Information Processing Systems*, 1999, p. 1029–1035.
- [13] G. Williams, P. Drews, B. Goldfain, J. M. Rehg, and E. A. Theodorou, "Information-theoretic model predictive control: Theory and applications to autonomous driving," *IEEE Transactions on Robotics*, vol. 34, no. 6, pp. 1603–1622, 2018.
- [14] N. A. Spielberg, M. Brown, and J. C. Gerdes, "Neural network model predictive motion control applied to automated driving with unknown friction," *IEEE Transactions on Control Systems Technology*, vol. 30, no. 5, pp. 1934–1945, 2022.
- [15] L. Hermansdorfer, R. Trauth, J. Betz, and M. Lienkamp, "End-to-end neural network for vehicle dynamics modeling," in *6th IEEE Congress on Information Science and Technology*, 2020, pp. 407–412.
- [16] N. A. Spielberg, M. Brown, N. R. Kapadia, J. C. Kegelman, and J. C. Gerdes, "Neural network vehicle models for high-performance automated driving," *Science Robotics*, vol. 4, no. 28, 2019.
- [17] A. Nagabandi, G. Kahn, R. S. Fearing, and S. Levine, "Neural network dynamics for model-based deep reinforcement learning with model-free fine-tuning," in *Proceedings of the IEEE International Conference on Robotics and Automation*, 2018, pp. 7559–7566.
- [18] A. Broad, I. Abraham, T. Murphey, and B. Argall, "Structured neural network dynamics for model-based control," *arXiv:1808.01184*, 2018.
- [19] F. Büning, A. Schalbetter, A. Aboudonia, M. H. de Badyn, P. Heer, and J. Lygeros, "Input convex neural networks for building MPC," in *Proceedings of the 3rd Conference on Learning for Dynamics and Control*, ser. Proceedings of Machine Learning Research, vol. 144, 2021, pp. 251–262.
- [20] H. Fang, N. Tian, Y. Wang, M. Zhou, and M. A. Haile, "Nonlinear Bayesian estimation: from Kalman filtering to a broader horizon," *IEEE/CAA Journal of Automatica Sinica*, vol. 5, no. 2, pp. 401–417, 2018.
- [21] G. Evensen and P. J. van Leeuwen, "An ensemble Kalman smoother for nonlinear dynamics," *Monthly Weather Review*, vol. 128, no. 6, pp. 1852 – 1867, 2000.
- [22] R. Rajamani, *Vehicle Dynamics and Control*. Springer US, 2012.